IEEE Open Journal of the Computer Society

Received 2 August 2023; accepted 27 August 2023. Date of publication 31 August 2023;
date of current version 4 October 2023. The review of this article was arranged by Associate Editor Songtao Guo.

Digital Object Identifier 10.1109/OJCS.2023.3310913

Co-Existence With IEEE 802.11 Networks in the ISM Band Without Channel Estimation

MUHAMMAD NAVEED AMAN [1] (Senior Member, IEEE), MUHAMMAD ISHFAQ [2], AND BIPLAB SIKDAR [3] (Senior Member, IEEE)

[1]School of Computing, University of Nebraska-Lincoln, Lincoln, NE 68588-0642 USA
[2]Department of Electrical Engineering, National University of Computer and Emerging Sciences, Peshawar 25000, Pakistan
[3]Department of Electrical and Computer Engineering, National University of Singapore, Singapore 117583

CORRESPONDING AUTHOR: MUHAMMAD NAVEED AMAN (e-mail: naveed.aman@unl.edu)

ABSTRACT Any new deployment of networks in the industrial, scientific, and medical (ISM) band, even though it is license-free, has to co-exist with IEEE 802.11 networks. IoT devices are typically deployed in the ISM band, creating a spectrum bottleneck for competing networks. This article investigates the issue of co-existence of wireless networks with WiFi networks. In our scenario, we consider WiFi as the "primary" or higher priority network co-existing with multiple "secondary" networks that may be used for low priority devices, with both networks operating in the ISM band. Towards this end, we first develop an analytical model for a metric called the "received symbol distance" at the primary receiver to obtain a power control parameter for secondary users. This power control parameter is used to scale the power of the secondary user according to the wireless channel between the primary transmitter and primary receiver. The proposed approach is computationally simple and does not require any estimation of channel coefficients. Simulation results show that the proposed technique can be used to effectively increase the spectrum utilization and the probability of a successful transmission by the secondary user, while not having any harmful effect on the primary user.

INDEX TERMS Co-existence, IEEE 802.11, wireless LAN, interference management.

I. INTRODUCTION

The demand for spectrum by wireless networks and the devices that use them has been growing over the last two decades. This demand has expanded dramatically with the emergence of the Internet of Things (IoT) and the predicted high number of devices. Unlicensed and licensed bands have spectrum shortage issues. There is an increasing demand for more spectrum resources in the unlicensed industrial, scientific, and medical band due to the expansion of IoT and wireless sensor applications, wireless local area networks (WLANs), Bluetooth, etc. As a result, equipment operating in unlicensed ISM bands incur severe co-channel interference, as well as additional channel impairments such as environmental noise and multipath propagation [1]. To decrease interference between several users, spread spectrum communications and transmit power limits by authorities like the Federal Communications Commission (FCC) [2] may help. However, dense network deployment is becoming more typical. In businesses and residences, for example, multiple human users share space with sensors and IoT devices. The users/devices may utilize different network access protocols (e.g., WiFi and Bluetooth), yet they share the same spectrum, raising the noise floor and lowering performance. Thus, solutions that allow multiple networks to coexist in the ISM band are crucial.

The most common design principle of modern wireless networks, including IEEE 802.11, is that only one communication per frequency band or channel is allowed at any given moment (CDMA is an exception). Interference from numerous nodes on the same frequency band renders the packets useless. Modern transceiver design has enhanced receiver robustness against inter-system interference. Transmitters can also adjust their parameters based on channel indication feedback and a secondary user can gain significant capacity through opportunistic spectrum access (OSA). Most of the existing work on concurrent transmission on the same channel involves techniques that require accurate estimation of the

channel coefficients. However, wireless channels are highly complex due to the wide range of factors that affect it and its highly dynamic nature. The channel coefficients in a wireless radio channel may be correlated in time, frequency, and space. Moreover, the mobility of transmitters, receivers, and scattering objects can cause the channel to change more rapidly, thereby making the task of channel estimation even more challenging. To solve this problem, we propose a technique which enables the concurrent sharing of a channel by multiple devices *without the need for complex channel estimation*.

IEEE 802.11 coexistence in the ISM band is a critical challenge in the context of the sustained growth of IoT applications. The availability of spectrum to offer network access to IoT devices is one of the key difficulties facing the IoT [3]. Because licensed spectrum is limited and expensive, the ISM band is an appealing alternative for IoT devices. Since IEEE 802.11 networks are prevalent in the ISM band, other networks, especially IoT networks, must coexist. In many circumstances, such as in homes and offices, IEEE 802.11 network users are given priority over other devices, such as temperature sensors. This article addresses such cases where IEEE 802.11 users have higher priority than coexisting networks. These circumstances are frequently explored in cognitive radios [4]. Cognitive radio allows a secondary user to access a primary user's spectrum (licensed or unlicensed) without affecting the primary user's communications. The primary problem in cognitive radio networks is balancing the competing objectives of secondary user performance and primary user interference.

This article focuses on a scenario where a primary IEEE 802.11 network (e.g., IEEE 802.11 versions a, g, n, ac) and multiple secondary networks (e.g., for low priority IoT devices) coexist. No assumption is made on the MAC protocol employed by the secondary network. The primary network may consist of multiple transmitters and receivers that have priority to use a specific frequency band (e.g., the 2.4 GHz ISM band). The secondary transmitters and receivers can use the channel only if they do not affect any ongoing transmissions in the primary network. The secondary transmitter may receive various forms of feedback from the primary receiver and adjust its transmission power to ensure that it does not cause unacceptable interference to the primary users. The *received symbol distance* is the distance between a received symbol and a reference symbol at a receiver. First, we build a mathematical model that captures the link between average received symbol distance (at the primary receiver) and secondary transmitter transmission power. Using this approach, we can derive a power control parameter that scales the secondary user's transmission power. This power control scheme prevents a secondary user's interference from affecting the primary users. This article's goal is to optimize secondary user throughput while minimizing primary network disturbance so that the primary network can function correctly. The following are the major contributions of this article:

- *Analytical model to characterize the Received Symbol Distance:* We derive a mathematical model to characterize interference in terms of a metric called received symbol distance. Using a realistic model for wireless communications, we derive an analytical expression that relates a power control parameter for a secondary transmitter to the average received symbol distance at the primary receiver.
- *Mechanism to enable concurrent transmissions with IEEE 802.11 networks:* We propose a mechanism to increase the throughput of secondary users by allowing concurrent transmissions on the same frequency as the primary users on a WiFi network. This mechanism scales the transmission power of the secondary users by using our analytical model for interference.
- *Performance evaluation:* We use extensive simulations to show that the proposed mechanism improves spectrum utilization by improving the throughput of secondary users while keeping the primary user unaffected.

The rest of the article is organized as follows. Section II provides a review of the related work. An analytical model for received symbol distance is derived in Section III. Section IV describes the proposed technique to allow concurrent transmissions from the secondary network to co-exist with the IEEE 802.11 network. We present the simulation results in Section V and conclude the article in Section VI.

II. LITERATURE REVIEW

A substantial body of work on finding the optimum channel and spectrum sensing for a cognitive network has been carried out in the past [5]. Recent works on co-existence of primary and secondary users using OSA include the following. The authors in [6] build a fundamental paradigm for analyzing neighboring channel co-existence by measuring the performance impact of nonlinearity in the receiver RF front-end. The authors in [7] proposed a machine learning based solution which enables secondary users to seek and opportunistically exploit the underutilized spectrum without interrupting the data transmission of primary users. Similarly, the authors in [8] proposed a deep learning-based spectrum opportunity detector in the 5 G/B5G cognitive radio (CR) network of IoTs and UAVs. Another technique for OSA based on primary user traffic patterns is proposed in [9]. OSA is modeled as a scheduling problem in [10]. The proposed technique uses an under average reward criterion with the Uniforming Random Ordered Policy (UROP) to achieve throughput-optimality. Similarly the authors in [1], formulate the spectrum access problem in the framework of Partially Observable Markov Decision Processes to obtain an average energy optimal policy. Underutilization of the ISM band in some places has motivated the development of unlicensed long-term evolution (LTE), combining LTE with Wi-Fi technologies [12], [15], [16], [17]. A summary of existing techniques is provided in Table 1.

The existing techniques for co-existence suffer from one or more of the following problems:

1) Transmit at a time when the primary network is silent or on frequency bands that are not being used by any of the primary users, limiting the performance gains that

TABLE 1. Summary of Existing Literature

Technique	Co-existence	Channel Estimation	SIC	Sensing
[7]	✓	✗	✓	✗
[8]	✓	✗	✓	✗
[10]	✗	✓	✓	✗
[9]	✗	✓	✓	✗
[1]	✗	✓	✗	✓
Proposed Technique	✓	✓	✓	✓

Co-existence: The proposed method exploits intervals when the primary network is silent.
Channel Estimation: The proposed method does not require channel estimation.
SIC: The proposed technique does not rely on SIC.
Sensing: The proposed method does not require accurate power sensing.

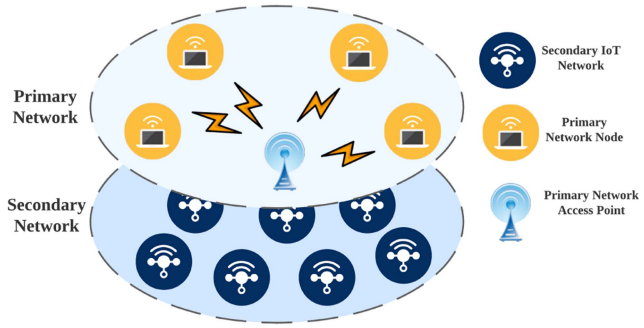

FIGURE 1. Network model.

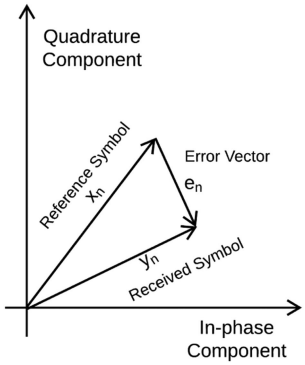

FIGURE 2. Received symbol distance definition.

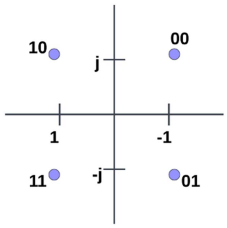

FIGURE 3. 4-QAM grey code constellation diagram.

can be achieved through co-existence and resulting in lower throughput for the secondary users.
2) Require accurate estimation of wireless channel co-efficients which makes these techniques difficult to implement.
3) Depend on SIC and if interference is high, then SIC may not work. Moreover, SIC increases the computation complexity, latency and energy requirements.
4) Depend on the estimation of path loss and accurate sensing of the power of the primary user.

Unlike existing techniques that rely on estimation of wireless channels, SIC, or accurate power sensing, the proposed technique is based an on analytical model of interference followed by solving an optimization problem to find the optimal transmit power for secondary users.

III. ANALYTICAL MODEL FOR RECEIVED SYMBOL DISTANCE

Our objective is to develop a metric that can easily capture the impact of secondary transmissions on the primary network. While the model is developed in the context of IEEE 802.11 based primary transmitter-receiver pairs, it is applicable to any network that uses OFDM as the physical layer.

The notations used in this article are given in Table 2. The network model or scenario studied in this article is shown in Fig. 1. We consider a primary IEEE 802.11 network and multiple secondary IoT networks. The transmitter and receiver in the primary network are denoted by T_p and R_p, while a pair of secondary transmitter and receiver is denoted by T_c and R_c, respectively. We assume that the secondary networks are located within the communication region of the primary network, and vice versa. Note that the primary network is considered to be the IEEE 802.11 network while the secondary network is considered to be any other wireless network using the same ISM band. Therefore, the primary and secondary networks typically do not communicate with each other.

We define the received symbol distance at the receiver as the difference between a received symbol and the reference symbol, as shown in Fig. 2. Note that when a packet is received, the symbols received are distorted due to noise, interference, or other propagation factors. Accordingly, the reference symbol for a received symbol is the ideal symbol, (i.e., without any noise or interference etc.) in the constellation to which it is decoded into. For example, the reference symbols for 4-QAM are shown in Fig. 3. y_n is the received equalized n-th symbol while x_n is the n-th reference symbol. We represent the received symbol distance as follows:

$$e_n = y_n - x_n \tag{1}$$

$$= (y_{R,n} - x_{R,n}) + j(y_{I,n} - x_{I,n}) \tag{2}$$

where $y_{R,n}$ and $y_{I,n}$ denote the real and imaginary parts of y_n, while $x_{R,n}$ and x_{I_n} denote the real and imaginary parts of x_n. Thus, we can also write the received symbol distance in terms of real and imaginary parts as follows:

$$e_n = e_{I,n} + je_{Q,n}.$$

TABLE 2. Notations

Notation	Description	Notation	Description
x_n	n-th reference symbol	y_n	received equalized n-th symbol
$x_{R,n}$	real part of x_n	$x_{I,n}$	Imaginary part of x_n
$y_{R,n}$	real part of y_n	$y_{I,n}$	Imaginary part of y_n
e_n	received symbol distance	$e_{R,n}$	real part of e_n
$e_{I,n}$	imaginary part of e_n	$\hat{x}_n$	estimate of x_n
$E[x]$	expected value of x	$x_p[n]$	transmitted symbols of the primary transmitter
$\alpha[n]$	channel fading coefficients for the primary channel	$\beta[n]$	fading coefficients for the secondary channel
$x_c[n]$	transmitted symbols of the secondary transmitter	$Z_p[n]$	AWGN in primary channel
$Z_c[n]$	AWGN in secondary channel	M	modulation order
σ^2	variance	η	power control parameter

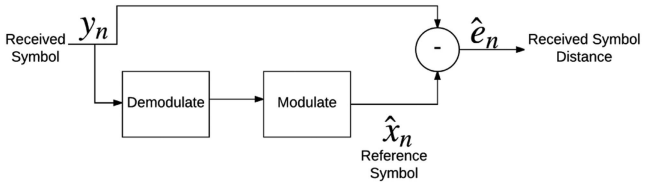

FIGURE 4. Received symbol distance calculation.

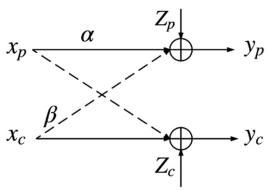

FIGURE 5. Channel model for primary and secondary links.

Let us define a random variable ζ as:

$$\zeta = \frac{1}{N}\sum_{n=0}^{N-1}|e_n|^2 \tag{3}$$

where ζ is measured over N symbols. We consider non-data aided receivers. Therefore, x_n needs to be estimated by demodulating y_n and then again modulating the result to obtain a reference symbol $\hat{x}_n$ as shown in Fig. 4.

The received symbol distance e_n is approximated by using the approximate value of x_n, i.e., $\hat{x}_n$. For large values of N, we have

$$\frac{1}{N}\sum_{n=0}^{N-1}|e_n|^2 \approx E\left[|\hat{e}_n|^2\right] = E\left[|y_n - \hat{x}_n|^2\right] \tag{4}$$

where $E[x]$ denotes the expected value of random variable x. If we assume quasi-static Rayleigh fading with the channel model given in Fig. 5, then the received signal for the primary receiver is represented by:

$$y_p[n] = \alpha[n]x_p[n] + \beta[n]x_c[n] + Z_p[n] \tag{5}$$

where $x_p[n]$ and $\alpha[n]$ represent the transmitted symbols of the primary transmitter and Rayleigh distributed random variables representing the channel fading coefficients for the primary channel, respectively. $x_c[n]$ and $\beta[n]$ represent the transmitted symbols and channel fading coefficients for the secondary networks, respectively, and given as follows:

$$\beta[n] = \left[\beta_{n,1}, \beta_{n,2}, \ldots, \beta_{n,I}\right], \tag{6}$$

$$x_c[n] = \left[x_{c,1}, x_{c,2}, \ldots, x_{c,I}\right]^T. \tag{7}$$

In the channel model shown in Fig. 5, $Z_p[n]$ and $Z_c[n]$ denote additive white Gaussian noise with variance σ_p^2 at the primary receiver and σ_c^2 at the secondary receivers, respectively. For analytical tractability, we initially take $\alpha[n] \approx 1$ and will reintroduce it later on. Moreover, for ease of notation we drop the index n for the rest of the analysis. Therefore, we can rewrite (5) as:

$$y_p = x_p + \beta x_c + Z_p. \tag{8}$$

The proposed scheme for interference avoidance depends on controlling the power of the secondary user. Therefore, we introduce an instantaneous power control parameter η into (8) as follows:

$$y_p = x_p + \sqrt{\eta}\beta x_c + Z_p \tag{9}$$

where $0 \leq \eta \leq 1$, and the value of η is dynamically adjusted according to the proposed power control strategy.

Let $x_{R,p}$ and $x_{I,p}$ denote the real and imaginary parts of x_p. Similar notations for y_p and x_c are used in this article. Equation (4) can be written in terms of the real and imaginary parts of the error vector as:

$$\begin{aligned} E\left[|\hat{e}|^2\right] &= E\left[|\hat{e}_R|^2\right] + E\left[|\hat{e}_I|^2\right] \\ &= E\left[|y_r - \hat{x}_{R,p}|^2\right] + E\left[|y_I - \hat{x}_{I,p}|^2\right]. \end{aligned} \tag{10}$$

For square quadrature amplitude modulation (QAM) signals, the independence and symmetry at the real and imaginary parts lead to $E[|\hat{e}_R|^2] = E[|\hat{e}_I|^2]$. Therefore, we can rewrite (10) as:

$$E[|\hat{e}|^2] = 2E\left[|y_r - \hat{x}_{R,p}|^2\right]. \tag{11}$$

This shows that to obtain the value of ζ, it is sufficient to only consider the real part of the signals.

When the number of subcarriers is large, the real and imaginary parts of x_p and x_c can be assumed to be independent and identically distributed Gaussian random variables with zero mean and variance of $\sigma_{x_p}^2$ and $\sigma_{x_c}^2$, respectively [13]. Then, the conditional probability density function of the received QAM

signal is given by:

$$f\left(y_{R,p}|x_{R,p}=S_i\right)=\frac{1}{\sigma_T}\phi\left(\frac{y_{R,p}-S_i}{\sigma_T}\right) \tag{12}$$

where σ_T is given by

$$\begin{aligned}\sigma_T &= \text{Var}\left[y_{R,p}|x_{R,p}=S_i\right]\\ &= \text{Var}\left[S_i+\sqrt{\eta}\beta x_c+Z_p\right]\\ &= \eta\beta^2\sigma_{x_c^2}+\sigma_p^2.\end{aligned} \tag{13}$$

Here, S_i is the value of the real part of the i-th transmitted symbol and $\phi(\cdot)$ represents the pdf of a standard normal distributed random variable. For QAM modulation, the real part of the symbols of x_p can be represented as:

$$x_{R,p}=(2i-k)d, \quad i=0,1,\ldots,k \tag{14}$$

where $k=\sqrt{M}-1$, with M being the modulation order. Moreover, the decision regions Δ_i for $x_{R,p}$, given a symbol S_i are

$$-\infty<\Delta_0\leq S_0+d, \quad \text{for } i=0 \tag{15}$$

$$S_i-d<\Delta_i\leq S_i+d, \quad \text{for } 1\leq i\leq k-1 \tag{16}$$

$$S_k-d<\Delta_k<\infty, \quad \text{for } i=k. \tag{17}$$

Now, to find $E[|y_r-\hat{x}_{R,p}|^2]$, we have

$$\begin{aligned}&E\left[|y_{R,p}-\hat{x}_{R,p}|^2\right]\\ &=\sum_{i=0}^{k}P\left(\hat{x}_{R,p}=S_i\right)E\left[(y_{R,p}-S_i)^2|\hat{x}_{R,p}=S_i\right]\\ &=\sum_{i=0}^{k}P\left(\hat{x}_{R,p}=S_i\right)\int_{-\infty}^{\infty}\left(y_{R,p}-S_i\right)^2\\ &\quad\times f\left(y_{R,p}|\hat{x}_{R,p}=S_i\right)dy_{R,p}.\end{aligned} \tag{18}$$

Assuming that all modulation symbols are transmitted with equal probability, we have

$$\begin{aligned}&P\left(\hat{x}_{R,p}=S_i\right)\\ &=\sum_{j=0}^{k}P\left(x_{R,p}=S_j\right)\int_{\Delta_i}\frac{1}{\sigma_T}\phi\left(\frac{y_{R,p}-S_j}{\sigma_T}\right)dy_{R,p}\\ &=\frac{1}{k+1}\sum_{j=0}^{k}P(x_{R,p}=S_j)\int_{\Delta_i}\frac{1}{\sigma_T}\phi\left(\frac{y_{R,p}-S_j}{\sigma_T}\right)dy_{R,p}.\end{aligned} \tag{19}$$

If we assume binary modulation with $x_{R,p}\in\{-d,d\}$ and $P(x_{R,p}=d)=P(x_{R,p}=-d)=1/2$, then we have

$$\begin{aligned}&f(y_{R,p}|\hat{x}_{R,p}=d)\\ &=\frac{1}{C}\left(f(y_{R,p}|x_{R,p}=d)+f(y_{R,p}|x_{R,p}=-d)\right), y_{R,p}>0\end{aligned} \tag{20}$$

$$\begin{aligned}&f\left(y_{R,p}|\hat{x}_{R,p}=-d\right)\\ &=\frac{1}{C}\left(f(y_{R,p}|x_{R,p}=d)+f(y_{R,p}|x_{R,p}=-d)\right), y_{R,p}<0.\end{aligned} \tag{21}$$

We can extend this to M-ary modulation by considering the decision regions in (15), (16), and (17) to obtain:

$$\begin{aligned}&f\left(y_{R,p}|\hat{x}_{R,p}=S_i\right)\\ &=\frac{1}{C_i}\left[\sum_{j=0}^{k}\frac{1}{\sigma_T}\phi\left(\frac{y_{R,p}-S_j}{\sigma_T}\right)\right], \quad y_{R,p}\in\Delta_i,\end{aligned} \tag{22}$$

where C_i is the normalization factor and can be calculated using:

$$\int_{-\infty}^{\infty}f\left(y_{R,p}|\hat{x}_{R,p}=S_i\right)dy_{R,p}=1 \tag{23}$$

which gives us:

$$C_i=\sum_{j=0}^{k}\int_{\Delta_i}\frac{1}{\sigma_T}\phi\left(\frac{y_{R,p}-S_j}{\sigma_T}\right)dy_{R,p}. \tag{24}$$

Using (19) and (22), (18) is reduced to:

$$E\left[|y_{R,p}-\hat{x}_{R,p}|^2\right]=\frac{1}{k+1}\sum_{i=0}^{k}\sum_{j=0}^{k}\int_{\tilde{\Delta}_i}\frac{\upsilon^2}{\sigma_T}\phi\left(\frac{\upsilon-\mu_{ji}}{\sigma_T}\right), \tag{25}$$

where $\upsilon=y_{R,p}-S_i$, $\tilde{\Delta}_i=\Delta_i-S_i$, and $\mu_{ji}=S_j-S_i=2d(j-i)$. Finally, it can be shown that [14]:

$$\begin{aligned}&E\left[|y_{R,p}-\hat{x}_{R,p}|^2\right]\\ &=\sigma_T^2-8d\sigma_T\sum_{i=1}^{k}\gamma_i\phi\left[\frac{\omega_i d}{\sigma_T}\right]+8d^2\sum_{i=1}^{k}\gamma_i\omega_i Q\left[\frac{\omega_i d}{\sigma_T}\right]\end{aligned} \tag{26}$$

where for better representation we denote $\gamma_i=1-\frac{i}{k+1}$, and $\omega_i=2i-1$.

Now we introduce α, i.e, the Rayleigh fading coefficient for the primary signals, into our analysis. Considering a normalized QAM system, we can represent d as:

$$d=\alpha\sqrt{\frac{3}{2(M-1)}}. \tag{27}$$

Thus, (26) can be written as:

$$\begin{aligned}&E\left[|y_{R,p}-\hat{x}_{R,p}|^2\right]\\ &=\sigma_T^2-8\sqrt{\frac{3\alpha^2\sigma_T^2}{2(M-1)}}\sum_{i=1}^{k}\gamma_i\phi\left[\sqrt{\frac{3\omega_i^2\alpha^2}{2\sigma_T^2(M-1)}}\right]\\ &\quad+\frac{12\alpha^2}{M-1}\sum_{i=1}^{k}\gamma_i\omega_i Q\left[\sqrt{\frac{3\omega_i^2\alpha^2}{2\sigma_T^2(M-1)}}\right].\end{aligned} \tag{28}$$

As the noise at the secondary transmitter is assumed to have zero mean, therefore we can consider $\sigma_{x_c}^2=P_c$, where P_c is the

signal power of a secondary user. A methodology to estimate $\sigma^2_{x_c}$ is presented in the Appendix. Moreover, using (4) and (28), we can rewrite (3) as:

$$\zeta(\alpha,\beta) = \delta - 8\sqrt{\frac{3\alpha^2\delta}{2(M-1)}}\sum_{i=1}^{\sqrt{M}-1}\gamma_i\phi\left[\sqrt{\frac{3\omega_i^2\alpha^2}{2\delta(M-1)}}\right] + \frac{12\alpha^2}{M-1}\sum_{i=1}^{\sqrt{M}-1}\gamma_i\omega_i Q\left[\sqrt{\frac{3\omega_i^2\alpha^2}{2\delta(M-1)}}\right], \quad (29)$$

where $\delta = \eta\beta^2 P_c + \sigma_p^2$. Exchanging the ϕ and Q functions in (29) with the exponential and error functions, respectively, we get

$$\zeta(\alpha,\beta) = \delta - 4\alpha\sqrt{\frac{3\delta}{\pi(M-1)}}\sum_{i=1}^{\sqrt{M}-1}\gamma_i e^{-\frac{3\omega_i^2\alpha^2}{2\delta(M-1)}} + \frac{6\alpha^2}{M-1}\sum_{i=1}^{\sqrt{M}-1}\gamma_i\omega_i \quad \text{erfc}\left(\sqrt{\frac{3\omega_i^2\alpha^2}{\delta(M-1)}}\right). \quad (30)$$

$\zeta(\alpha,\beta)$ can be considered as the instantaneous value for ζ for a given α and β. To find the expected value of ζ, we average (30) over α and β. The pdfs of α and β are given by

$$f(\alpha) = 2\alpha e^{-\alpha^2}, \quad \alpha \geq 0$$
$$f(\beta) = 2\beta e^{-\beta^2}, \quad \beta \geq 0.$$

Taking the average of (30) over α, we get (31) shown at the bottom of this page. Similarly, taking the expectation of (31) over β, we get (32) shown at the bottom of the next page, where Ω_i is given by

$$\Omega_i = \frac{3(2i-1)^2}{2(M-1)}. \quad (33)$$

Note that the purpose of these transformations is to obtain the average received symbol distance in terms of the power control parameter η from (30) which gives the instantaneous value for ζ for a given α and β. We use ζ in Section IV to develop our interference avoidance mechanism.

IV. INTERFERENCE AVOIDANCE MECHANISM FOR SECONDARY USERS

In this section we describe the proposed mechanism for interference avoidance and improving the coexistence of secondary wireless networks with IEEE 802.11 based networks, by allowing concurrent transmissions from a secondary user on the same frequency channel. The proposed interference avoidance protocol is shown in Fig. 6.

A secondary network should satisfy two criteria in order to co-exist with an IEEE 802.11 network: i) it should not impede the contention mechanism of the IEEE 802.11 nodes, and ii) it should not interfere with any ongoing IEEE 802.11 transmissions. These objectives can be achieved by appropriate carrier sensing and power control (by choosing the parameter η) at the secondary transmitter. Our objective here is to present a general methodology for co-existence rather than a specific protocol. An exact protocol for use in the secondary network is beyond the scope of this article.

The flow diagram and algorithm to be followed at the primary receiver are shown in Fig. 7(a) and Algorithm 1,

$$\begin{aligned}\zeta(\beta) &= \int_0^\infty \zeta(\alpha,\beta)f(\alpha)\mathrm{d}\alpha \\ &= \int_0^\infty \left(\eta\beta^2P_c + \sigma_p^2 - 4\alpha\sqrt{\frac{3(\eta\beta^2P_c+\sigma_p^2)}{\pi(M-1)}}\sum_{i=1}^{\sqrt{M}-1}\gamma_i e^{-\frac{3\omega_i^2\alpha^2}{2(\eta\beta^2P_c+\sigma_p^2)(M-1)}} + \frac{6\alpha^2}{M-1}\sum_{i=1}^{\sqrt{M}-1}\gamma_i\omega_i \quad \text{erfc}\left(\sqrt{\frac{3\omega_i^2\alpha^2}{\left(\eta\beta^2P_c+\sigma_p^2\right)(M-1)}}\right)2\alpha e^{-\alpha^2}\right)\mathrm{d}\alpha \\ &= \eta\beta^2P_c + \sigma_p^2 - 4(\eta\beta^2P_C+\sigma_p^2)^2\sqrt{\frac{3}{2(M-1)}}\sum_{i=1}^{\sqrt{M}-1}\gamma_i\left(\frac{3\omega_i^2}{2(M-1)} + (\eta\beta^2P_c+\sigma_p^2)\right)^{-\frac{3}{2}} \\ &\quad + \frac{6}{M-1}\sum_{i=1}^{\sqrt{M}-1}\gamma_i\omega_i\left[1 - \frac{1}{2}\sqrt{\frac{3\omega_i^2}{\left(\eta\beta^2P_c+\sigma_p^2\right)(M-1)}}\left(\frac{6\omega_i^2\alpha^2}{\left(\eta\beta^2P_c+\sigma_p^2\right)(M-1)} + 3\right)\right. \\ &\quad \left.\left(\frac{3\omega_i^2\alpha^2}{\left(\eta\beta^2P_c+\sigma_p^2\right)(M-1)} + 1\right)^{-\frac{3}{2}}\right]. \end{aligned} \quad (31)$$

Algorithm 1: Interference Avoidance at Primary Receiver.

Input : ζ_{max}, σ_p^2, M
Output: η
P_m = Receive New Packet
Calculate ζ
if $\zeta \geq \zeta_{max}$ **then**
  // Calculate the new power scaling factor η
  Estimate P_c
  Calculate η using Equation (35)
  Send η to Secondary Transmitter
else
  Send P_m to upper layers

respectively. Similarly, the flow diagram and algorithm to be followed at secondary transmitters are shown in Fig. 7(b) and Algorithm 2, respectively. We now describe the operation of the primary and secondary networks in detail.

A. OPERATION OF THE PRIMARY NETWORK

In the proposed framework for co-existence with IEEE 802.11 networks, no changes are required at the primary IEEE 802.11 transmitters. Thus, transmitters in the IEEE 802.11 networks follow the usual CSMA/CA mechanism specified in the standards (e.g. [21] for IEEE 802.11a). However, the primary receivers aid the secondary network with their power control. Other than this, no change is required to the IEEE 802.11 receiver.

As shown in Fig. 7(a) and Algorithm 1, when a packet is received at the primary receiver, it first calculates its average received symbol distance ζ. If ζ is less than the maximum threshold given in Table 3, the primary transmitter is not affected by interference and can continue its operation. However, if the ζ value is greater than the threshold, the secondary transmitter needs to scale its transmit power and accordingly adjust its data rate. For this purpose, the primary receiver inputs P_c, σ_p^2 and the current maximum threshold value of ζ from Table 3 into (35), to obtain the maximum permissible value of η. The primary receiver then sends this η value to the secondary transmitter.

The primary network uses IEEE 802.11 as the MAC protocol. Thus, all feedbacks and network operation must be compatible with IEEE 802.11's protocol and message structures. Consequently, the η value to be communicated to the secondary transmitter is inserted into the reserved portion of the "duration" field of a frame that follows the frame structure of an ACK packet specified by the IEEE 802.11 standard [21], as shown in Fig. 8. This enables the proposed framework for co-existence to work without any modification to the IEEE 802.11 frame structures.

$$
\begin{aligned}
\zeta &= \int_0^\infty \zeta(\beta) f(\beta) \mathrm{d}\beta \\
&= \int_0^\infty \left(\eta\beta^2 P_c + \sigma_p^2 - 4(\eta\beta^2 P_C + \sigma_p^2)^2 \sqrt{\frac{3}{2(M-1)}} \sum_{i=1}^{\sqrt{M}-1} \gamma_i \left(\frac{3\omega_i^2}{2(M-1)} + (\eta\beta^2 P_c + \sigma_p^2) \right)^{-\frac{3}{2}} \right. \\
&\quad + \frac{6}{M-1} \sum_{i=1}^{\sqrt{M}-1} \gamma_i \omega_i \left[1 - \frac{1}{2} \sqrt{\frac{3\omega_i^2}{(\eta\beta^2 P_c + \sigma_p^2)(M-1)}} \left(\frac{6\omega_i^2 \alpha^2}{(\eta\beta^2 P_c + \sigma_p^2)(M-1)} + 3 \right) \right. \\
&\quad \left. \left. \left(\frac{3\omega_i^2 \alpha^2}{\left(\eta\beta^2 P_c + \sigma_p^2\right)(M-1)} + 1 \right)^{-\frac{3}{2}} \right] 2\beta e^{-\beta^2} \right) \mathrm{d}\beta \\
&= \eta P_c + \sigma_p^2 + 8 \sqrt{\frac{3}{2(M-1)}} \sum_{i=1}^{\sqrt{M}-1} \gamma_i \frac{1}{4\eta P_c \sqrt{\Omega_i^2 + \sigma_p^2}} \\
&\quad \left[(\eta^2 P_c^2 - 4\eta P_c \Omega_i - 4\Omega_i^2) e^{\frac{\Omega_i + \sigma_p^2}{\eta P_c}} \sqrt{\frac{\Omega_i + \sigma_p^2}{\eta P_c}} \left(\sqrt{\pi}\,\mathrm{erf}\left(\sqrt{\frac{\Omega_i + \sigma_p^2}{\eta P_c}} \right) - \sqrt{\pi} \right) - 2\eta P_c (\Omega_i + \sigma_p^2) - 4\Omega_i^2 \right] \\
&\quad - \frac{3}{(M-1)^{3/2} (\eta P_c)^{3/2}} \sum_{i=1}^{\sqrt{M}-1} \gamma_i \omega_i \sqrt{\frac{3\omega_i^2}{3\omega_i^2 + 2\sigma_p^2 (M-1)}} \left[(3\omega_i^2 + 3\eta P_c (M-1)) \sqrt{2\pi (3\omega_i^2 + 2\sigma_p^2 (M-1))} \right. \\
&\quad \left. e^{\frac{3\omega_i^2}{2\eta P_c (M-1)} + \frac{\sigma_p^2}{\eta P_c}} \,\mathrm{erf}\left(\sqrt{\frac{3\omega_i^2 + 2\sigma_p^2 (M-1)}{2\eta P_c (M-1)}} + 6\omega_i^2 \sqrt{\eta P_c (M-1)} \right) \right]
\end{aligned}
\tag{32}
$$

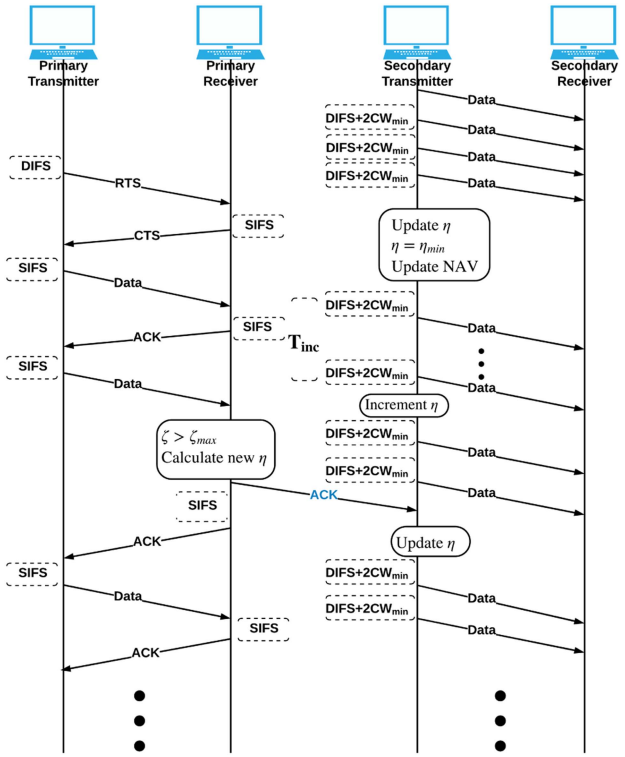

FIGURE 6. Interference avoidance protocol.

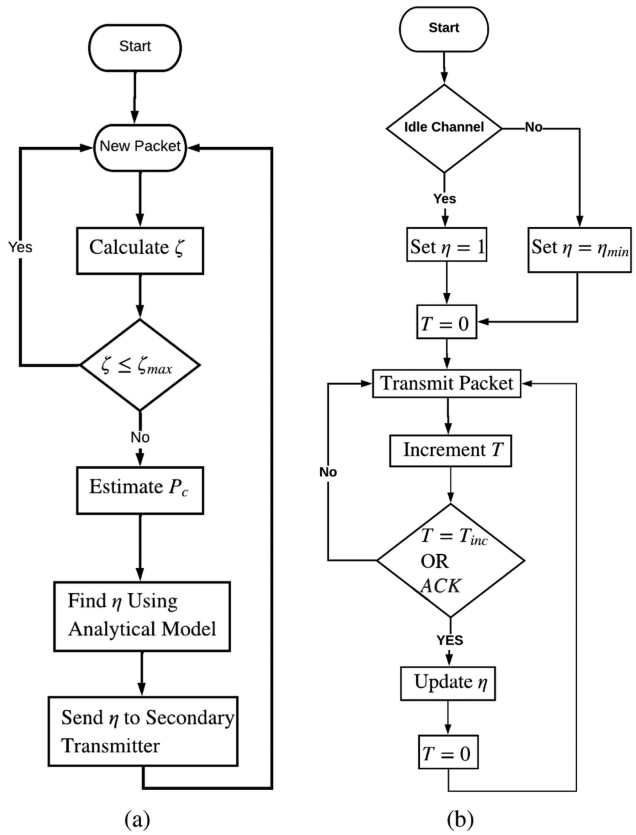

FIGURE 7. Interference avoidance.

Algorithm 2: Interference Avoidance at Secondary Transmitter.

Input : η_{min}, T_{inc}
Output: η

```
Sense Channel
if queue length == 0 then
    // Set η to maximum value i.e., 1
    η = 1
T = 0
while (queue length > 0) do
    Transmit Packet
    T = T+1
    if T == T_inc AND η < 1 then
        η = max{η + 0.05, 1}
        T = 0
    else if ACK Received then
        // Set η to the value received from
           the Primary Receiver
        η = η_ACK
        T = 0
    else if RTS sent by Primary Transmitter then
        // Set η to the minimum value
        η = η_min
        T = 0
end
```

TABLE 3. Maximum ζ for IEEE 802.11a Data Rates

Data Rate (Mbps)	ζ_{max}	Data Rate (Mbps)	ζ_{max}
6	0.3162	9	0.1585
12	0.1	18	0.0501
24	0.0251	36	0.0126
48	0.0063	54	0.0032

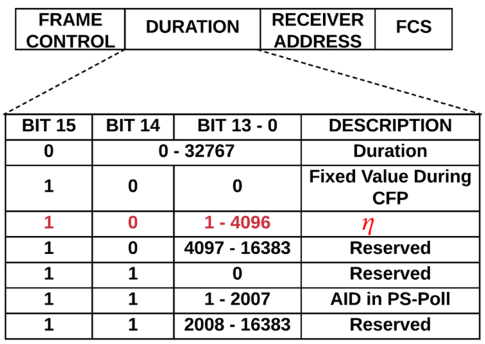

BIT 15	BIT 14	BIT 13 - 0	DESCRIPTION
0	0 - 32767		Duration
1	0	0	Fixed Value During CFP
1	0	1 - 4096	η
1	0	4097 - 16383	Reserved
1	1	0	Reserved
1	1	1 - 2007	AID in PS-Poll
1	1	2008 - 16383	Reserved

FIGURE 8. IEEE 802.11 ACK frame with reserved field used to carry η value.

The objective of the proposed framework is to facilitate the co-existence with IEEE 802.11 networks while maximizing the throughput of the secondary user. To achieve this objective, the secondary transmitter should use the largest possible transmit power (using the power control parameter η) without creating unacceptable levels of interference in the primary network. As shown in Section III, the impact of the secondary transmitter on the primary network can be modeled through the received symbol distance metric, ζ. The maximum tolerable values of ζ for the unhindered operation of the

primary network for various data rates of IEEE 802.11a, denoted by $\zeta_{\max}$, as obtained using the framework in Section III are given in Table 3, [18], [21].

In order to allow secondary users to effectively transmit their data, the power control parameter η should be as large as possible. Thus, we formulate the problem of selecting η as our primal optimization problem as follows:

$$\begin{aligned} \max_{\zeta_{\max}, P_c, \sigma_p^2} : \quad & \eta \\ \text{subject to:} \quad & a) \quad \zeta - \zeta_{\max} \leq 0, \\ & b) \quad \eta - 1 \leq 0. \end{aligned}$$

Here, the first constraint ensures that the impact of the secondary transmission stays below the maximum acceptable level of distortion in the received symbol at the primary receiver. To find the optimal solution for this problem, we define a Lagrangian function as:

$$L(\eta, \mu_1, \mu_2) = \eta - \mu_1 (\zeta - \zeta_{\max}) - \mu_2(\eta - 1). \tag{34}$$

Solving for the optimal value of η from (34), we get (35) shown at the bottom of this page. The readers are referred to [22] for further details on how to solve a constrained optimization problem using Lagrange functions. The expression for the optimal power control parameter as obtained in (35) is used by the primary receiver and secondary transmitter (as described in Section IV-B and IV-A) for facilitating secondary transmissions in the presence of IEEE 802.11 networks.

B. OPERATION OF THE SECONDARY NETWORK

The secondary network's operation is guided by two principles: i) ensure that its transmissions do not create an unacceptable level of interference in the IEEE 802.11 network and ii) exploit all opportunities to transmit in order to maximize its throughput. These objectives are achieved by transmit power control and opportunistic channel access, respectively.

Before transmitting a packet, the secondary transmitter first checks if the channel is idle. Note that the secondary transmitter may proceed with a transmission even if the channel is busy, as long as it uses a sufficiently low transmit power. The secondary transmitter deems the channel to be idle if no activity is detected for a period of $DIFS + 2CW_{\min}$ where $DIFS$ represents the distributed inter-frame space and $CW_{\min}$ is the minimun contention window for devices in the IEEE 802.11 network. Note that the secondary transmitter may choose to wait for a period of $DIFS + CW_{\max}$ to be absolutely sure that no primary transmitter is contending for the channel (where $CW_{\max}$ is the maximum contention window). However this is undesirable and inefficient because i) IEEE 802.11 nodes are in their maximum backoff stage very rarely under normal circumstances [19] and ii) the conservative choice of the secondary transmitter's transmit power makes the likelihood of intereference at the primary receiver very low. Once the waiting time of $DIFS + 2CW_{\min}$ is over, the secondary transmitter proceeds with its transmission based on the current value of the power control parameter η. The methodology for updating η is given in Section IV-B1.

The deferral of transmission by the secondary transmitter for a period of $DIFS + 2CW_{\min}$ serves two purposes. Firstly, it avoids any interference with the backoff mechanism of the primary IEEE 802.11 devices. Secondly, it ensures that the secondary transmitter can overhear any acknowledgment (ACK) packet sent by the primary receiver. It also provides a high likelihood of overhearing the start of any new data or RTS transmission in the primary network. Also, in cases where the secondary transmitter begins its transmission after overhearing an RTS or data packet from the primary transmitter, it limits its length of transmission to be short enough so that it can overhear the ACK packet that will be transmitted in the primary network. While these measures may not always guarantee that the secondary transmitter will overhear the ACKs in the primary network, the emphasis on the ability to hear such ACKs is because they carry the information on the acceptable η values.

1) SECONDARY TRANSMIT POWER CONTROL

In order to estimate the appropriate value of η to use for a packet transmission, the secondary transmitter monitors the activity of the IEEE 802.11 primary network. The secondary transmitter continuously updates its η estimate while it has packets to send (i.e., its MAC layer packet queue is non-empty). The secondary transmitter resets the value of η to one when its MAC layer queue becomes empty.

During the periods when its MAC layer queue is non-empty, the secondary transmitter updates its estimate of η as follows. The secondary transmitter first initializes a counter T to zero. For every packet that it sends, the secondary transmitter increments T by one. It then updates η at each of the following events:

- *RTS/Data received:* If the secondary transmitter overhears a new request to send (RTS) frame or a data frame (without any preceding RTS frame) from the IEEE 802.11 transmitter, it adjusts η to the minimum value, i.e., $\eta_{\min}$.
- *Counter T reaches threshold T_{inc}:* Due to the possibility of changing channel characteristics and to probe for the maximum allowable value of η, the secondary transmitter attempts to opportunistically increase the transmit power after a period of T_{inc}. If the secondary transmitter sends T_{inc} packets without any explicit indication

$$\eta\left(\zeta_{\max}, P_c, \sigma_p^2\right) = \frac{3}{P_c}\sqrt{\frac{6\pi M^2 P_c^2 - 12\pi\zeta_{\max}^2 M P_c^2 + 12\pi M P_c + 6\pi\zeta_{\max} P_c^2 - 12\pi P_c + 6\pi\sigma_p^2}{(M-1)P_c^3}} \tag{35}$$

from the primary receiver to decrease η, the secondary transmitter multiplicatively increases its transmit power. Thus, each time T reaches T_{inc} the secondary transmitter increments η by 0.05 and this in turn causes an increase of 5% in its transmit power.

- *ACK received:* When the interference at the IEEE 802.11 receiver increases above the defined threshold value, it sends out an ACK frame with a new η value destined for the secondary transmitter as described previously. If the secondary transmitter overhears an ACK frame from the primary receiver, it updates η and scales its transmit power according to the new η value.

Note that in the proposed strategy, the secondary transmitter reverts to the minimum transmit power, i.e., $\eta_{\min}$ whenever it overhears a RTS or data packet from a primary transmitter. This is because there may be multiple nodes (each a primary transmitter) in an IEEE 802.11 network and the same value of η may not be acceptable for all IEEE 802.11 nodes. In addition, nodes may be mobile and accordingly their acceptable η values may change over time. Thus, the secondary transmitter resets its η to the minimum value to allow for any IEEE 802.11 device to communicate without being affected by the secondary transmitter.

The parameter T_{inc} determines the frequency at which the value of η is adjusted by the secondary transmitter. At moderate and high loads, WiFi nodes transmit data frequently and a secondary transmitter may not be able to send more than one or two packets between two successive WiFi packets. Thus, we use $T_{inc} = 2$ in the proposed mechanism. Also, our simulations showed that an η value of 0.1 causes negligible interference in almost all practical deployment scenarios. Therefore, a value of 0.1 is used for $\eta_{\min}$ in this article.

Finally, we note that it is possible that the transmission from the secondary transmitter causes an error in the reception of the primary receiver. As per the IEEE 802.11 protocol, the receiver only sends out ACKs in the case of successful receptions. Moreover, the primary transmitter may be a hidden terminal for the secondary transmitter. Thus, in these cases, the secondary transmitter would not be updated with the correct value of η to use. To address this situation, in cases where the secondary transmitter does not overhear an ACK from the primary after its transmission (but it is aware of the RTS/CTS or data transmission), it will conservatively revert to using $\eta_{\min}$ for the next packet.

V. RESULTS

In this section we present the simulation results to evaluate the proposed framework for co-existence and interference avoidance and compare the performance with related work in existing literature. The scenario shown in Fig. 1 was simulated using Matlab and Simulink. The simulations use the standard IEEE 802.11 modulation related and timing related parameters [21], as shown in Tables 4 and 5, respectively.

In our simulations, the IEEE 802.11 primary transmitter transmitted at a constant data rate, while the secondary transmitter used adaptive modulation to adjust its data rate. We evaluated the proposed protocol under two SNR scenarios: high SNR and low SNR, and three data rates: 36 Mbps, 48 Mbps, and 54 Mbps. We consider high SNR as 35 dB for 36 Mbps, and 38 dB for 48/54 Mbps [21]. Similarly, a low SNR corresponds to 25 dB and 28 dB for 36 Mbps and 48/54 Mbps, respectively [21].

TABLE 4. Modulation Parameters

Data rate (Mbits/s)	Modulation	Coding rate (R)	Coded bits per sub-carrier (N_{BPSC})	Coded bits per OFDM symbol (N_{CBPS})	Data bits per OFDM symbol (N_{DBPS})
6	BPSK	1/2	1	48	24
9	BPSK	3/4	1	48	36
12	QPSK	1/2	2	96	48
18	QPSK	3/4	2	96	72
24	16QAM	1/2	4	192	96
36	16QAM	3/4	4	192	144
48	64QAM	2/3	6	288	192
54	64QAM	3/4	6	288	216

TABLE 5. Timing Related Parameters

Parameter	Value
N_{SYM}: Samples per OFDM symbol	80
N_{FFT}: FFT Length	64
N_{SD}: Number of data subcarriers	48
N_{SP}: Number of pilot subcarriers	4
N_{ST}: Number of total subcarriers	52 ($N_{SD} + N_{SP}$)
N_{TRAIN}: Number of training symbols	2
Δ_F: Subcarrier frequency spacing	0.3125 MHz (=20 MHz/64)
T_{FFT}: IFFT/FFT period	3.2μs($1/\Delta_F$)
$T_{PREAMBLE}$: Preamble duration	8μs
T_{GI}: Guard Interval (GI) duration	0.8μs ($T_{FFT}/4$)
T_{GI2}: Training symbol GI duration	8μs
T_{SYM}: Symbol interval	4μs ($T_{GI} + T_{FFT}$)
T_{LONG}: Training sequence duration	8μs ($T_{GI2} + 2xT_{FFT}$)

To evaluate the proposed scheme's coexistence and ability to exploit the nature of a fading channel, we place the transmitter and receiver pairs for the IEEE 802.11 and secondary users close to each other. The IEEE 802.11 transmitter and receiver are separated by a distance of 1 m. The distance between the secondary transmitter and receiver is also 1 m. The distance between the primary transmitter and secondary receiver, and secondary transmitter and primary receiver is initially taken as 5 meters. However, we slowly move the secondary network away from the primary network and check the performance of both networks in terms of the probability of success and throughput. We define the probability of success P_s as follows:

$$P_s = \frac{\text{Number of packets received successfully}}{\text{Total number of packets transmitted}}. \quad (36)$$

A higher probability of success is interpreted as better performance. As a benchmark, we compare the proposed mechanism with the most relevant state-of-the-art works on co-existence of wireless networks in the ISM band by Kim

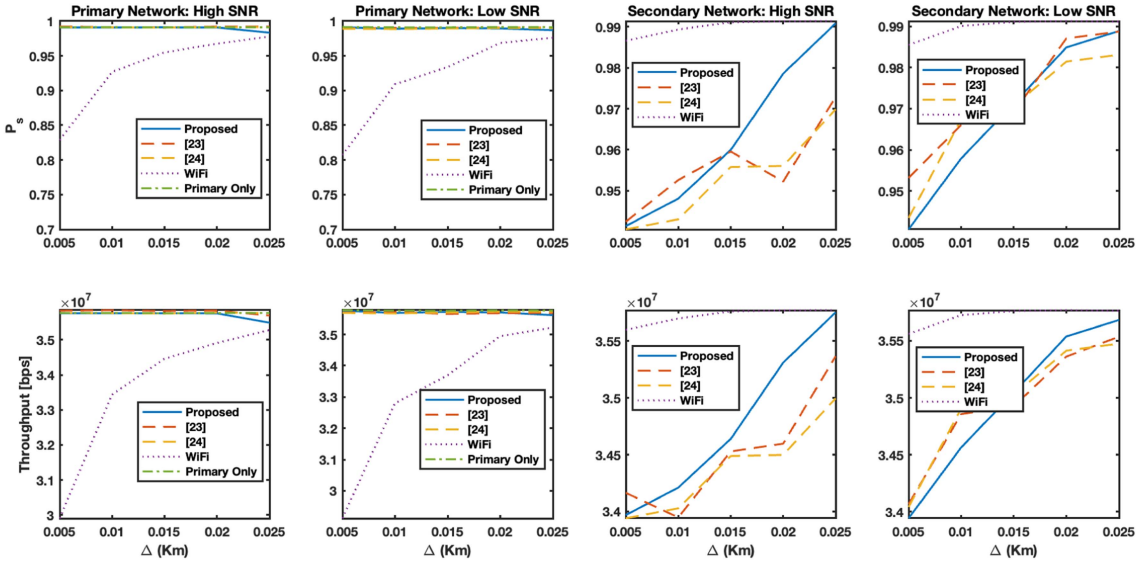

FIGURE 9. Performance comparison, data rate: 36 Mbps.

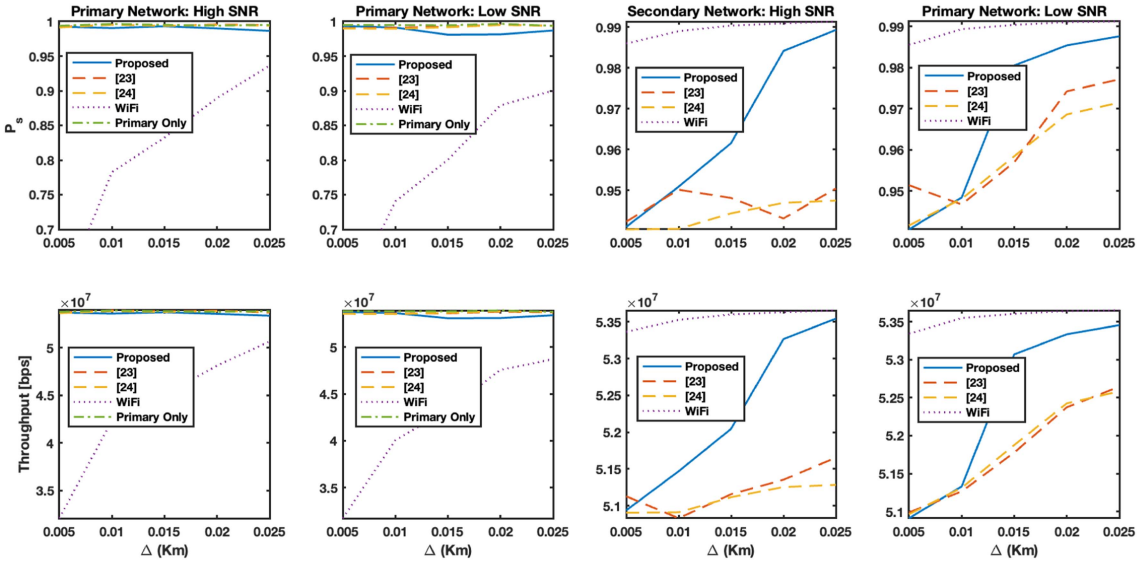

FIGURE 10. Performance comparison, data rate: 54 Mbps.

et al. [23] and Tao et al. [24]. The authors of [23] propose a two phase strategy by combining probabilistic collision avoidance with dynamically changing the channel access method. The objective of the technique proposed by Kim et al. [23] is to maximize throughput of multiple co-existing wireless networks. The authors of [24] propose an opportunistic power control strategy based on the signal to interference plus noise ratio (SINR) at the primary receiver. The technique proposed in [24], solves the problem of achieving maximum throughput for the secondary network while providing a communication guarantee to the primary user as an optimization problem using the SINR. We also give results for the case when the primary and secondary networks are not using any interference avoidance and the case when the secondary network does not exist, labeled as *WiFi* and *Primary Only*, respectively, in Figs. 9 and 10. Our objective is to maximize P_s and the throughput for the secondary network, while keeping the P_s and throughput of the primary IEEE 802.11 network unaffected. Figs. 9 and 10 show the performance of the IEEE 802.11 network, with high SNR and low SNR at the primary and secondary networks for two choices of data rates at the primary IEEE 802.11 network: 36 and 54 Mbps, respectively. For each choice of the data rate of the primary network, the secondary network uses the adaptive data rate strategy of IEEE 802.11a.

Figs. 9, 10 and Table 6 show that P_s and the throughput for the IEEE 802.11 network stays approximately unaffected for the proposed mechanism as well as [23] and [24]. However,

TABLE 6. Primary Network Throughput Comparison for a Separation of 5 m, 15 m and 25 m Between the Primary and Secondary Network

Data Rate	SNR	Primary Only	Proposed Technique						[23]						[24]					
			5m		15m		25m		5m		15m		25m		5m		15m		25m	
			T (Mbps)	D (%)	T (Mbps)	D (%)	T (Mbps)	D (%)	T (Mbps)	D (%)	T (Mbps)	D (%)	T (Mbps)	D (%)	T (Mbps)	D (%)	T (Mbps)	D (%)	T (Mbps)	D (%)
36 Mbps	High	35.77	35.76	0	35.76	0	35.49	0.75	35.44	0.92	35.35	1.14	35.35	1.14	35.77	0	35.77	0	35.76	0
	Low	35.76	35.76	0	35.72	0.11	35.62	0.39	35.50	0.73	35.49	0.76	35.51	0.70	35.69	0.19	35.7	0.17	35.73	0
48 Mbps	High	47.62	47.48	0.29	47.23	0.82	47.08	1.1	47.15	0.99	47.18	0.92	47.20	0.88	47.58	0	47.62	0	47.56	0.12
	Low	47.61	47.47	0.29	47.20	0.86	47.09	1.09	47.10	1.07	47.15	0.97	47.05	1.18	47.48	0.27	47.47	0.29	47.42	0.40
54 Mbps	High	53.79	53.71	0.14	53.74	0	53.38	0.76	53.60	0.35	53.75	0.07	53.75	0.07	53.65	0.26	53.78	0	53.79	0
	Low	53.78	53.77	0	53.09	1.2	53.41	0.68	53.58	0.37	53.67	0.20	53.79	0	53.57	0.39	53.67	0.2	53.77	0

T: throughput, D: percent degradation.

TABLE 7. Secondary Network Throughput Comparison for a Separation of 5 m, 15 m and 25 m Between the Primary and Secondary Network

Data Rate	SNR	5m					15m					25m				
		Proposed Technique	[23]		[24]		Proposed Technique	[23]		[24]		Proposed Technique	[23]		[24]	
		T (Mbps)	T (Mbps)	I (Mbps)	T (Mbps)	I (Mbps)	T (Mbps)	T (Mbps)	I (Mbps)	T (Mbps)	I (Mbps)	T (Mbps)	T (Mbps)	I (Mbps)	T (Mbps)	I (Mbps)
36 Mbps	High	33.97	33.45	0.52	33.94	0.03	34.64	34.60	0.04	34.49	0.15	35.75	35.49	0.26	35.00	0.75
	Low	34.04	33.90	0.14	33.94	0.10	35.05	34.95	0.08	35.03	0.02	35.68	35.51	0.17	35.47	0.21
48 Mbps	High	45.28	45.25	0.03	45.24	0.04	47.16	45.25	1.91	45.26	1.9	47.64	45.80	1.84	45.77	1.87
	Low	45.26	45.25	0.01	45.26	0	47.25	45.98	1.27	46.15	1.1	47.55	46.80	0.75	46.82	0.73
54 Mbps	High	50.94	51.15	0	50.90	0.04	52.04	51.15	0.89	51.11	0.93	53.54	51.72	1.82	51.28	2.26
	Low	50.96	50.95	0.01	50.91	0.05	53.07	51.84	1.23	51.88	1.19	53.45	52.59	0.86	52.58	0.87

T: throughput, I: improvement.

the primary network suffers from a poor P_s in the absence of any interference avoidance. Moreover we observe that the P_s of the proposed mechanism outperforms that of [23] and [24] at higher data rates, i.e., the P_s for the secondary network is better. Similarly, these figures also show that the throughput obtained by the secondary network using the proposed mechanism is also higher than [23] and [24]. We observe that as the separation between the primary and secondary networks increases, the proposed technique clearly outperforms [23] and [24] at higher data rates as shown in Table 7. Moreover, the technique proposed in [23] incurs additional overhead due to switching between different channel access methods while the technique proposed in [24] requires acquisition of β, i.e., the channel coefficients of the secondary user, which is a difficult task. The simulation results presented here were obtained by assuming zero switching overhead for [23] and providing the exact channel coefficients to the model of [24]. We note that the introduction of estimation errors will further degrade the performance of [24]. This shows that the performance of the proposed mechanism is better. Moreover, the effects of fading, path loss, and shadowing etc. weaken the signal of the secondary transmitter. As expected intuitively, it can also be observed from Figs. 9 and 10 that the effect of interference from the secondary network on the IEEE 802.11 primary network is reduced as the secondary network moves away from the primary network.

VI. CONCLUSION

This article presented a framework for interference avoidance in wireless networks and showed that a secondary network can co-exist with an IEEE 802.11 based primary network by scaling the transmission power of the secondary user. We show that by using the received symbol distance as a design metric, it is possible to increase the throughput of a secondary network without affecting the IEEE 802.11 primary network, even when both networks use the same channel concurrently. We observe that due to the effects of fading and path loss, the co-existence of the two networks improves when the distance between the two networks increases.

The results presented in this article are for the IEEE 802.11a protocol. However, the proposed technique is based on systems employing OFDM at the physical layer. Therefore, the proposed technique can be adopted by any system using OFDM. The analytical model used in this article considers a single secondary network. As part of the future work, the analytical model can be extended to model multiple secondary users.

APPENDIX

To calculate $\sigma_{x_c}^2$, we start by calculating the average symbol distance for the training symbols in a received packet at the primary receiver. Since the receiver knows the training symbols, the average symbol distance is given by

$$\zeta_T = \frac{1}{T}\sum_{n=0}^{T-1}|e_n|^2 = \frac{1}{T}\sum_{n=0}^{T-1}\left|\alpha x_n + \beta x_c + Z_p - x_n\right|^2. \quad (37)$$

After applying channel estimation and equalization at the receiver, we can assume $\alpha = 1$. Thus,

$$\begin{aligned}\zeta_T &= \frac{1}{T}\sum_{n=0}^{T-1}|x_n + \beta x_c + Z_p - x_n|^2 \\ &= \frac{1}{T}\sum_{n=0}^{T-1}|\beta x_c + Z_p|^2 \end{aligned} \quad (38)$$

and for large T, we have

$$\frac{1}{T}\sum_{n=0}^{T-1}|\beta x_c + Z_p|^2 = \varepsilon\left\{|\beta x_c + Z_p|^2\right\}. \quad (39)$$

Therefore, we can re-write (38) as follows:

$$\begin{aligned}\zeta_T &= \varepsilon\left\{|\beta x_c + Z_p|^2\right\} \\ &= \beta^2\varepsilon\left\{x_c^2\right\} + \varepsilon\left\{Z_p^2\right\} + 2\beta\varepsilon\left\{x_c\right\}\varepsilon\left\{Z_p\right\} \\ &= \beta^2\sigma_{x_c}^2 + \sigma_p^2. \end{aligned} \tag{40}$$

Averaging (40) over β, we get

$$\begin{aligned}\zeta_T &= \int_0^\infty \left(\beta^2\sigma_{x_c}^2 + \sigma_p^2\right) 2\beta e^{-\beta^2} \mathrm{d}\beta \\ &= \sigma_{x_c}^2 + \sigma_p^2. \end{aligned} \tag{41}$$

Therefore, to find $\sigma_{x_c}^2$ we can use

$$\sigma_{x_c^2} = \zeta_T - \sigma_p^2 \tag{42}$$

where ζ_T is calculated over the training symbols and σ_p^2 is provided by the transmitter.

REFERENCES

[1] M. Santhoshkumar and K. Premkumar, "Energy-efficient opportunistic spectrum access in multichannel cognitive radio networks," *IEEE Netw. Lett.*, vol. 5, no. 1, pp. 1–5, Mar. 2023.

[2] "Title 47 of the CFR," Code of Federal RegulaNons, Accessed: May, 20, 2023. [Online]. Available: https://www.ecfr.gov/current/title-47

[3] A. Rajandekar and B. Sikdar, "A survey of MAC layer issues and protocols for machine-to-machine communications," *IEEE Internet Things J.*, vol. 2, no. 2, pp. 175–186, Apr. 2015.

[4] J. Mitola and G. Q. Maguire, "Cognitive radio: Making software radios more personal," *IEEE Pers. Commun.*, vol. 6, no. 4, pp. 13–18, Aug. 1999.

[5] N. H. S. Adam, "Spectrum sharing in cognitive radio networks with quality of service awareness," M. Sc Thesis, United Arab Emirates Univ., Al Ain, UAE, May 2015.

[6] A. V. Padaki, R. Tandon, and J. H. Reed, "On adjacent channel coexistence with receiver nonlinearity," *IEEE Trans. Wireless Commun.*, vol. 17, no. 7, pp. 4922–4936, Jul. 2018.

[7] P. Zhu, J. Li, D. Wang, and X. You, "Machine-learning-Based opportunistic spectrum access in cognitive radio networks," *IEEE Wireless Commun.*, vol. 27, no. 1, pp. 38–44, Feb. 2020.

[8] R. Ahmed, Y. Chen, and B. Hassan, "Deep learning-driven opportunistic spectrum access (OSA) framework for cognitive 5G and beyond 5G (B5G) networks," *Ad Hoc Networks*, vol. 123, 2021, Art. no. 102632.

[9] K. Arshid et al., "Primary user traffic pattern based opportunistic spectrum handoff in cognitive radio networks," *Appl. Sci.*, vol. 10, no. 5, 2020, Art. no. 1674.

[10] O. M. Gul, "Near-optimal opportunistic spectrum access in cognitive radio networks in the 5G and IoT era," in *Proc. IEEE 46th Conf. Local Comput. Netw.*, 2021, pp. 403–406.

[11] E. M. Ghourab, L. Bariah, S. Muhaidat, P. C. Sofotasios, M. Al-Qutayri, and E. Damiani, "Reputation-aware relay selection with opportunistic spectrum access: A blockchain approach," *IEEE Open J. Veh. Technol.*, vol. 4, pp. 389–403, 2023.

[12] Y. Yang, K. Hiltunen, and F. Chernogorov, "On the performance of coexistence between public eMBB and non-public URLLC networks," in *Proc. IEEE 93rd Veh. Technol. Conf.*, 2021, pp. 1–6.

[13] F. Yang et al., "Nondata-aided error vector magnitude analysis of $\eta - \mu$ fading channels in device-to-device communications," *IEEE Access*, vol. 7, pp. 82101–82109, 2019.

[14] H. A. Mahmoud and H. Arslan, "Error vector magnitude to SNR conversion for non-data-aided receivers," *IEEE Trans. Wireless Commun.*, vol. 8, no. 5, pp. 2694–2704, May 2009.

[15] A. Al-Dulaimi, S. Al-Rubaye, Q. Ni, and E. Sousa, "5G communications race: Pursuit of more capacity triggers LTE in unlicensed band," *IEEE Veh. Technol. Mag.*, vol. 10, no. 1, pp. 43–51, Mar. 2015.

[16] C. Chen, R. Ratasuk, and A. Ghosh, "Downlink performance analysis of LTE and WiFi coexistence in unlicensed bands with a simple listen-before-talk scheme," in *Proc. IEEE 81st Veh. Technol. Conf.*, 2015, pp. 1–5.

[17] F. M. Abinader et al., "Enabling the coexistence of LTE and Wi-Fi in unlicensed bands," *IEEE Commun. Mag.*, vol. 52, no. 11, pp. 54–61, Nov. 2014.

[18] M. N. Aman, W. K. Chan, and B. Sikdar, "Collision detection in IEEE 802.11 networks by error vector magnitude analysis," in *Proc. IEEE Glob. Commun. Conf.*, 2012, pp. 5218–5223.

[19] A. Rajandekar and B. Sikdar, "O-MAC: Opportunistic MAC protocol for M2M communication in WiFi white spaces," *IEEE Commun. Lett.*, vol. 21, no. 11, pp. 2440–2443, Nov. 2017.

[20] A. Bildea, "Link quality in wireless sensor networks," Ph.D. Thesis, Sch. Math., Inf. Sci. Technol., Comput. Sci., Universite de Grenoble, Grenoble, France, 2013.

[21] *IEEE Standard for Information Technology–Telecommunications and Information Exchange between Systems Local and Metropolitan Area Networks–Specific Requirements Part 11: Wireless LAN Medium Access Control (MAC) and Physical Layer (PHY) Specifications Amendment 1: Enhancements for High-Efficiency WLAN*, IEEE Standard 802.11ax-2021 (Amendment to IEEE Standard 802.11-2020), pp. 1–767, 19 May 2021.

[22] D. P. Bertsekas, *Constrained Optimization and Lagrange Multiplier Methods*, 1st ed. New York, NY, USA: Academic Press, 1996.

[23] B. Kim, J. H. Choi, and J. Cho, "A hybrid channel access scheme for coexistence mitigation in IEEE 802.15.4–based WBAN," *IEEE Sensors J.*, vol. 17, no. 21, pp. 7189–7195, Nov. 2017.

[24] Z. Tao, Y. Qin, H. Zhang, and S. Kuo, "Adaptive power control for mutual interference avoidance in industrial Internet-of-Things," *IEEE China Commun.*, vol. 13, no. 1, pp. 124–131, 2016.

MUHAMMAD NAVEED AMAN (Senior Member, IEEE) received the B.Sc. degree in computer systems engineering from KPK UET, Peshawar, Pakistan, the M.Sc. degree in computer engineering from CASE, Islamabad, Pakistan, the M.Eng. degree in industrial and management engineering and the Ph.D. degree in electrical engineering from Rensselaer Polytechnic Institute (RPI,) Troy, NY, USA, in 2006, 2008, and 2012, respectively. He is currently an Assistant Professor with the University of Nebraska-Lincoln, Lincoln, NE, USA. His research interests include IoT security and wireless networks.

MUHAMMAD ISHFAQ received the B.Sc. degree in electrical engineering from the Comsats University, Islamabad, Pakistan, in 2011 and the M. Sc. degree in electrical engineering from the National University of Computer and Emerging Sciences, Peshawar, Pakistan, in 2017 His research interests include wireless network, spectrum sharing, and cognitive radio networks.

BIPLAB SIKDAR (Senior Member, IEEE) received the B.Tech. degree in electronics and communication engineering from North Eastern Hill University, Shillong, India, in 1996, the M.Tech. degree in electrical engineering from IIT, Kanpur, India, in 1998, and the Ph.D. degree in electrical engineering from Rensselaer Polytechnic Institute (RPI), Troy, NY, USA, in 2001. He is currently a Professor with the Department of Electrical and Computer Engineering, National University of Singapore, Singapore. His research interests include wireless network, and security for IoT, and cyber physical systems.